Conformational Stability of 1-Butene: An Electron Momentum Spectroscopy Investigation

Fang Wu,[†] Xiangjun Chen,*[,†] Xu Shan,[†] Shan Xi Tian,[‡] Zhongjun Li,[†] and Kezun Xu[†]

Hefei National Laboratory for Physical Sciences at Microscale, Department of Modern Physics, and Department of Chemical Physics, University of Science and Technology of China, Hefei, 230026, People's Republic of China

Received: November 9, 2007; In Final Form: February 18, 2008

The valence-shell electron momentum distributions for 1-butene are measured by electron momentum spectroscopy (EMS) employing non-coplanar symmetric geometry. The experimental electron momentum distributions are compared with the density functional theory (DFT) calculations using different-sized basis sets. Although the two conformers of 1-butene in the gas phase, namely the skew and syn, have very close ionization potentials, the electron momentum distributions, especially in the low momentum region, can show prominent differences for some of the valence orbitals. By comparing the experimental electron momentum profiles with the theoretical ones, the skew conformer is found to be more stable than the syn and their relative abundances at room temperature are estimated to be (69 ± 6)% and (31 ± 6)%, respectively. It demonstrates that EMS has the latent potential to study the relative stability of conformers.

I. Introduction

The isomeric or conformational phenomena indwells numerous molecules from simple inorganic compounds up to large biomolecules (e.g., nucleic acid bases),[1−9] and their relative stabilities have attracted a great deal of theoretical and experimental interest because of the significantly different stereochemical reactivities.[10−30] 1-Butene, one of the simplest alkenes, has been theoretically predicated[16] existing four low-lying conformers: skew, syn, anti, and gauche. However, only skew and syn conformers have been confirmed by the experiments,[31−37] and the precise nature of the equilibrium between skew and syn conformers of 1-butene has not been determined. Extensive works have been performed to investigate the enthalpy differences between the skew and syn and the relative conformational abundances by means of far-infrared,[31] Raman,[32] microwave spectroscopy (MW),[33] mid-infrared,[34] NMR,[35−37] and various theoretical calculations (e.g., CBS-Q, G2).[16] Two contradictory conclusions of the syn−skew conformational stability have been derived. By the microwave spectroscopy,[33] the skew conformer was suggested more stable than the syn and had a small enthalpy difference of 0.15 ± 0.15 kcal/mol with respect to the syn conformer, while the Raman,[32] infrared,[31,34] and NMR spectra[35−37] argued that the syn conformer was a little more energetically favorable, and the enthalpy of syn conformer was lower by 0.22 kcal/mol (Raman), 0.1 ± 0.05 kcal/mol (NMR) in the liquid phase, and 0.209 ± 0.017 kcal/mol (IR) in gas phase than the skew. Furthermore, theoretical calculation studies[16,19−21] all predicated that the skew conformer is the favorable one.

Most of the previous experimental and theoretical studies focused on determining the relative abundance between the skew and syn conformers in the energetic domain. Besides the energetic differences among the conformers, the conformational effects can also be reflected by the variance of the molecular electronic structures. Namely, the different methyl orientations in the syn and skew conformers can lead to the different spatial electron density distributions for certain molecular orbitals (MOs). Electron momentum spectroscopy (EMS) is an experimental technique that can effectively probe the electron density distributions in momentum space for individual atomic and molecular orbitals.[38] Thus by comparing the measured electron momentum profiles with the calculated ones for conformational structures, it is possible to determine the Boltzmann-weighted abundances and thus the relative stability for different conformers.

In the earlier years, EMS was used to investigate the isomeric effect of isobutene, *cis*-2-butene, *trans*-2-butene, and isodichloroethylene and its cis, trans isomers by Leung and his co-workers.[39−42] Subsequently, the conformational effect was considered for the first time in the EMS study on electron structures for valence orbitals of glycine by Brion and his coworkers.[43,44] More recently, EMS studies by Deleuze et al.,[45] Wang et al.,[46] and Yang et al.[47] have shown that EMS is a feasible experimental method to study the conformational preference of molecules. In this article, the first EMS study for the valence orbitals of 1-butene has been carried out by using an energy dispersive multichannel (e, 2e) electron momentum spectrometer employing symmetric non-coplanar geometry. The relative conformational stability of 1-butene has been determined by comparing the theoretical and experimental momentum profiles. The energy and momentum resolution of the present EMS spectrometer is determined to be ∼1.1 eV (full width at half-maximum (fwhm)) and 0.15 au, respectively, by measuring Ar 3p ionization.

II. Experimental and Theoretical Background

The details of the present EMS spectrometer have been given elsewhere.[48] Briefly, the gas-phase target molecules are ionized by impact with a high-energy incident electron beam (1200 eV + binding energy). The scattered and ionized electrons are energetically selected (∼600 eV) by two hemispherical electron energy analyzers and detected in coincidence by microchannel plate position sensitive detectors. In the non-coplanar symmetric geometry, the polar angles of the two analyzers are kept fixed

* Corresponding author. Fax: 86-551-3606266. E-mail: xjun@ustc.edu.cn.
[†] Department of Modern Physics.
[‡] Department of Chemical Physics.

10.1021/jp710757y CCC: $40.75
Published on Web 05/01/2008

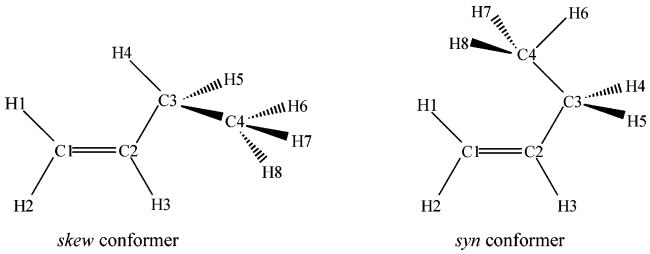

Figure 1. Schematic geometries for the skew and syn conformers of 1-butene.

at $\theta_1 = \theta_2 = \theta = 45°$ and the relative azimuthal angle ϕ between them is variable over wide range ($0° \sim \pm 30°$) by rotating one analyzer around the incident electron beam and keeping another one fixed. Because of the clean "knock-out" collision in which the residual ion acts as a spectator, the magnitude of the target electron momentum is related to the azimuthal angle ϕ by[38]

$$p = \{(2p_1 \cos\theta - p_0)2 + [2p_1 \sin\theta \sin(\phi/2)]^2\}^{1/2} \quad (1)$$

where p_0 and p_1 are the momenta of the incident and outgoing electrons, respectively.

Within the plane wave impulse approximation (PWIA) and target Hartree−Fock approximation (THFA) or Kohn−Sham approximation (TKSA), the triple differential cross-section (TDCS) σ_{EMS} for randomly oriented molecules can be described as[38,49]

$$\sigma_{\mathrm{EMS}} \propto S_q^{(f)} \int \mathrm{d}\Omega_p |\varphi_q(\mathbf{p})|^2 \quad (2)$$

where $\varphi_q(\mathbf{p})$ is the one-electron momentum space canonical HF or KS wavefunction for the qth MO from which the electron ejected. $S_q^{(f)}$ is the spectroscopic factor or pole strength that is the possibility of forming a one-hole configuration in the final ion state $|f\rangle$. The integral in eq 2 is known as the spherically averaged electron momentum distribution or electron momentum profile.

The skew and syn conformers of 1-butene are two equilibrium positions when the methyl group undergoes the internal rotation around the middle C−C single bond, as illustrated in Figure 1. The geometries of the two conformers are optimized by using the second-order Møllet−Plesset perturbation (MP2) method with aug-cc-pVTZ basis sets. The geometric parameters are in good agreement with the previous values by microwave spectroscopy.[33] The potential energy curve for rotation about the middle C−C single bond for 1-butene were calculated at the G2 and CBS-Q theoretical levels by Murcko et al.[16] The two minima at CCCC dihedral angles of 0 and 119° were found to be syn and skew, respectively. The syn−skew Gibbs free energy differences ΔG and enthalpy differences ΔH at room temperature (298 K) calculated by G2 and CBS-Q methods are 0.40 and 0.30 kcal/mol and 0.47 and 0.37 kcal/mol, respectively, while the syn−skew barrier is about 1.5 kcal/mol (G2) and 2.2 kcal/mol (CBS-Q).[16]

The theoretical momentum profiles (TMPs) for the valence orbitals of the skew and syn conformers of 1-butene have been calculated within THFA or TKSA according to eq 2. The corresponding position space orbital wavefunctions are calculated using Hartree−Fock (HF) and density functional theory (DFT) methods with different-sized basis sets of 6-311++G, 6-311G**, 6-311++G**, cc-pVTZ and aug-cc-pVTZ by GAUSSIAN 03 program.[50] For DFT calculations, B3LYP hybrid functional is employed that refers to Becke's three parameters hybrid functional using Lee−Yang−Parr correlation functional.[51] The calculated results indicated that no obvious difference can be observed for TMPs of 1-butene calculated by the HF and B3LYP method when employing the same basis set, therefore only the B3LYP calculations using different-sized basis sets will be presented in the present article. To compare with the experiments, the instrumental momentum (i.e., angular) resolution is folded into the TMPs using the Gaussian-weighted planar grid (GWPG) method.[52]

III. Results and Discussions

A. Binding Energy Spectra. The skew and syn conformers of 1-butene belong to the C_1 and C_s point group symmetries, respectively. Both HF and B3LYP calculations give the ground-state electronic configurations as

$$(core)^8 \underbrace{(1a)^2(2a)^2(3a)^2(4a)^2}_{inner-valence} \underbrace{(5a)^2(6a)^2(7a)^2(8a)^2(9a)^2(10a)^2(11a)^2(12a)^2}_{outer-valence}$$

for the skew conformer and

$$(core)^8 \underbrace{(1a')^2(2a')^2(3a')^2(4a')^2}_{inner-valence} \underbrace{(5a')^2(1a'')^2(6a')^2(7a')^2(2a'')^2(8a')^2(9a')^2(3a'')^2}_{outer-valence}$$

for the syn conformer.

The 32-electron molecule of 1-butene has 12 individual valence orbitals. The calculations of ionization potentials (IPs) for the outer valence orbitals of 1-butene have been performed using B3LYP, the outer valence Green's function (OVGF) method,[53] and the partial third-order electron propagator (P3)[54] method with 6-311++G** basis set. The results are listed in Table 1. For OVGF and P3 methods, the pole strengths can also be obtained and listed in the square brackets. OVGF and P3 models assign MOs based on HF wavefunctions. It is noted that the HF calculation only contains the exchange energy resulting from the electronic fermion nature, while in the DFT calculation, not only the exchange energy but also the correlation effect are included. Hence, in some cases, they may yield different ordering of MOs in IPs.[55] As mentioned in last section, no obvious differences can be observed for TMPs of 1-butene calculated by the HF and B3LYP method when employing the same basis sets for the same numbers of MOs, indicating that B3LYP model yield the same ordering of MOs as OVGF and P3 models for the present molecule of 1-butene.

As can be seen in Table 1, the corresponding valence orbitals of the skew and syn conformers have approximately the equal IPs and present the same ionization band in the binding energy spectra (BES). Previous experimental works on the ionizations of 1-butene comprise the HeI ultraviolet photoelectron spectroscopy (UPS)[56] and the synchrotron radiation photoelectron spectroscopy (SRPES).[57] The experimental IPs for 1-butene are presented in Table 2. The conformational effect was not taken into account in the PES works[56,57] and the assignments were made according to the symmetry of the syn conformer. Compared with the experiments, the OVGF and P3 calculations give more consistent IPs in the outer valence region than B3LYP method.

The BES in the range of 5−30 eV have been measured at 15 different relative azimuthal angles (ϕ): 1, 2, 3, 4, 5, 6, 7, 8, 9, 11, 13, 15, 17, 19, and 24°. The ones at the $\phi = 1$ and 9° are

TABLE 1: Theoretical Results of the Ionization Potentials (eV) for the skew and syn Conformers of 1-butene

orbitals	OVGF/6-311++G**[a]		P3/6-311++G**[a]		B3LYP/6-311++G**[b]	
skew/syn	skew	syn	skew	syn	skew	syn
12*a*/3*a*″	9.67 [0.91]	9.68 [0.91]	9.67 [0.91]	9.65 [0.91]	7.06	7.07
11*a*/9*a*′	11.89 [0.91]	11.93 [0.91]	11.86 [0.90]	11.85 [0.90]	9.24	9.24
10*a*/8*a*′	12.44 [0.91]	12.40 [0.92]	12.24 [0.90]	12.37 [0.91]	9.49	9.67
9*a*/2*a*″	12.81 [0.92]	13.05 [0.91]	12.98 [0.90]	12.62 [0.91]	10.26	9.79
8*a*/7*a*′	13.76 [0.91]	13.53 [0.91]	13.41 [0.90]	13.59 [0.90]	10.53	10.76
7*a*/6*a*′	14.58 [0.90]	14.78 [0.90]	14.63 [0.90]	14.57 [0.90]	11.70	11.71
6*a*/1*a*″	15.33 [0.90]	15.18 [0.90]	15.07 [0.89]	15.33 [0.90]	12.16	12.36
5*a*/5*a*′	16.12 [0.87]	16.07 [0.88]	16.12 [0.87]	15.94 [0.87]	12.92	13.11
4*a*/4*a*′	18.24 [0.86]	18.67 [0.86]			15.21	14.79
3*a*/3*a*′					17.24	17.60
2*a*/2*a*′					19.95	19.93
1*a*/1*a*′					21.86	21.99

[a] Pole strengths calculated by P3 and OVGF are all listed in square brackets. [b]Based on Koopmann's theorem.

TABLE 2: Experimental Results of the Ionization Potentials (eV) for 1-butene

EMS[a]		He I UPS[56]		SRPES[57]	
(12*a*/3*a*″)	10.0	(3*a*″)	10.0	(3*a*″)	9.8
(11*a*+10*a*+9*a*+8*a* /9*a*′+8*a*′+2*a*″+7*a*′)	12.0	(9*a*′+8*a*′+2*a*″)	12.0		11.9
	13.4	(7*a*′)	13.4	(9*a*′,8*a*′,2 *a*″ ,7*a*′	13.0
(7*a*+6*a*+5*a* /6*a*′+1*a*″+5*a*′)	14.8	(6*a*′)	14.8	6*a*′, 1*a*″,5*a*′)	15.1
	15.9	(5*a*′)	15.9		15.8
(4*a*/4*a*′)	18.3	(1*a*″)	17.8	(4*a*′)	18.2
(3*a*/3*a*′)	20.6		(3*a*′)		20.5
(2*a*/2*a*′)	22.8		(2*a*′)		22.6
(1*a*/1*a*′)	24.7		(1*a*′)		24.4

[a] This work.

displayed in Figure 2. Because the energy resolution of the present EMS cannot resolve all the 12 ionization bands for individual valence orbitals, only nine Gaussian peaks (p1−p9 in Figure 2) are fitted to the BES as shown by dashed curves. The width for each Gaussian peak is determined by the EMS instrumental energy resolution (1.1 eV in the present work) convoluting the Frank−Condon widths of the corresponding bands observed in the He I UPS[56] (p1−p6) and in the SRPES[57] (p7−p9). The positions of the Gaussian peaks are determined by the IPs reported by the high-resolution PES experiments[56,57] and indicated by the vertical bars in Figure 2. For inner valence orbitals, we adjusted peak positions a little to best fit the present experimental BES. The overall fitted spectra are represented by the solid lines.

As shown in Figure 2, the first band (p1) at 10.0 eV is well resolved and corresponds to the ionization of the highest occupied molecular orbital (HOMO) of 1-butene, that is, 12*a* orbital of the skew conformer and 3*a*″ orbital of the syn conformer (noted as 12*a*/3*a*″ in the following discussions). The next two bands located at 12.0 eV (p2) and 13.4 eV (p3) cannot be well resolved with respect to the energy resolution of the spectrometer. He I UPS work assigned the p2 to the ionizations of 9*a*′, 8*a*′, and 2*a*″ orbitals (noted as 9*a*′ + 8*a*′ + 2*a*″ in the following discussions) and p3 to 7*a*′ orbital where only the syn conformer was taken into account.[56] Next two bands at 14.8 eV (p4) and 15.9 eV (p5) also overlap each other due to the low-energy resolution of EMS. He I UPS work assigned the p4 to the ionization of 6*a*′ orbital and p5 to 5*a*′, while assigned the sixth bands (p6) at ∼18.2 eV to 1*a*″.[56] On the other hand, the SRPES experiment[57] assigned the p6 to the ionization of 4*a*′ orbital. As can be seen in Table 1, according to the present theoretical calculations including OVGF, P3 and B3LYP methods, it is more likely to assign the band p6 to ionization of 4*a*′/4*a*, and the bands p4 and p5 to the ionizations of 6*a*′ + 1*a*″/7*a* + 6*a* (p4) and 5*a*′/5*a* (p5). The assignments of these three bands will be investigated by comparing their TMPs with the experiments in Section III. B. The last three bands located at 20.6 (p7), 22.8 (p8), and 24.7 eV (p9) correspond to ionizations of the three innermost valence orbitals, that is, 3*a*/3*a*′, 2*a*/2*a*′, and 1*a*/1*a*′. The present experimental IPs by EMS for 1-butene are presented in Table 2, together with the results of He I UPS[56] and SRPES[57] works.

B. Experimental and Theoretical Momentum Profiles. Nine Gaussian peaks corresponding to the ionizations from 12 valence orbitals of 1-butene are fitted to the BES. The experimental momentum profile (XMP) for each Gaussian peak is extracted by deconvoluting the same peak from the sequentially obtained BES at different azimuthal angles ϕ and plotting area under the corresponding fitted peaks as a function of momentum p (i.e., ϕ angle). Because p2 and p3, p4, and p5 are not well resolved because of the small energy spacing, their individual momentum profiles are scattered and not reliable. Thus only the summed momentum profiles for p2 + p3 and p4 + p5 are reported in this work.

The XMPs for the valence orbitals of 1-butene are shown as solid circles in Figure 3a−g, together with the TMPs calculated using B3LYP method with 6-311++G, 6-311G**, 6-311++G**, cc-pVTZ, and aug-cc-pVTZ basis sets. The XMPs and TMPs are placed on a common intensity scale by normalizing the TMP to the XMP for HOMO (12*a*/3*a*″). This is reasonable because the pole strengths for HOMO are very close to unity according to the OVGF and P3 calculations. Because 1-butene coexists in two conformers, the Boltzmann-weighted abundances should be taken into account when comparing the XMPs with theoretical calculations. The detailed discussions of the relative abundances for the two conformers of 1-butene will be given in Section III. C. Relative abundances of (69 ± 6)% for the skew and (31 ± 6)% for the syn conformers have been deduced and employed in the discussions in the present section. In Figure 3a−g, the total TMPs are the summation of the respective TMPs, 69% for the skew and 31% for the syn conformers. The individual TMPs for the skew (dashed line) and syn (dotted line) conformers calculated by B3LYP/aug-cc-pVTZ are also shown in figures (multiplied by the respective relative abundances). And the orbital density surface plots in position space calculated by B3LYP/ aug-cc-pVTZ for the two conformers are displayed on the right-hand side of the figures for some orbitals.

The XMP and TMPs for HOMO are shown in Figure 3a, together with the orbital density surface plots of the skew and syn conformers. It can be seen that the electron densities for 12*a* and 3*a*″ orbitals mainly distribute on the C═C double bond and exhibit typical π-orbitals. Therefore the rotation of the methyl group has little influence on the electron momentum distribution for HOMO. Both of the individual TMPs for the

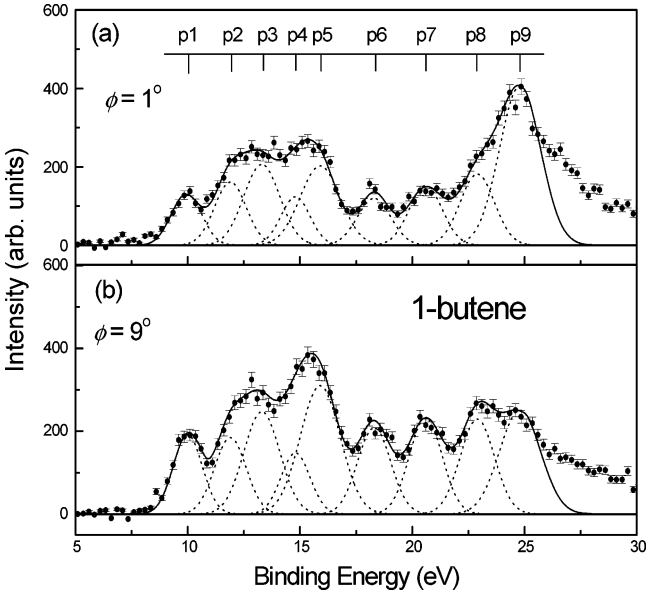

Figure 2. Binding energy spectra (BES) of 1-butene at (a) $\phi = 1°$, (b) $\phi = 9°$. The dotted lines represent the Gaussian peaks fitting the BES. The solid line is the summed fit. The vertical bars indicate the positions of the Gaussian peaks.

two conformers exhibit "p-type" in nature only with different maximum positions at $p \sim 0.45$ au for the skew and $p \sim 0.57$ au for the syn conformers. The XMP for HOMO also shows the expected p-type character (a maximum position at $p \sim 0.58$ au) but with a strong "turn up" in the low momentum region below 0.25 au. Previous research studies indicated that such turn up for π orbital in the low momentum region can be ascribed to the distorted-wave effect.[58−60] The TMPs calculated by B3LYP method with 6-311++G, 6-311++G** and aug-cc-pVTZ basis sets which include "diffuse" functions predict higher intensity in low momentum region and a smaller maximum position at ~ 0.53 au than XMP. While the TMPs calculated by B3LYP method with 6-311G** and cc-pVTZ basis sets which do not include "diffuse" function predict a maximum position at ~ 0.59 au and are in better agreement with XMP. Among all the TMPs, the B3LYP/cc-pVTZ provides the best description of the experiment.

The summed XMP and TMPs for p2 and p3 ($11a + 10a + 9a + 8a/9a' + 8a' + 2a'' + 7a'$) are shown in Figure 3b. It can be seen that the XMP exhibits an "sp-type" character with a minimum at $p \sim 0.32$ au and a secondary maximum at $p \sim 0.65$ au All the calculations roughly reproduce the shape whereas largely underestimate the experimental data in the region from $p \sim 0.25$ to ~ 0.9 au. Among all the calculations, B3LYP with 6-311++G** and aug-cc-pVTZ give the best fit in the low momentum region $p < 0.25$ au. The high intensity in the low momentum region in XMP may partly be ascribed to the distorted-wave effect because $11a$, $9a$, $9a'$ and $2a''$ are π*-like orbitals.

The difference between the individual TMPs for the skew and syn conformers can clearly be observed as shown in Figure 3b. The TMP for the skew exhibits "sp-type" character, whereas the TMP for the syn is mainly "p-type" in nature.

Figure 3c compares the summed XMP and TMPs for p4 and p5 ($7a + 6a + 5a/ 6a' + 1a'' + 5a'$). Generally, all the summed TMPs well reproduce the XMP both in shape and intensity. A significant difference between the individual TMPs for the two conformers can be observed. The TMP for the skew exhibits a "p-type" character with a maximum at $p \sim 0.55$ au, while the TMP for the syn is mainly "s-type" in nature. As mentioned in Section III. A, He I UPS work assigned p4 + p5 to $6a' + 5a'$ for the syn conformer,[56] while the theoretical calculations give different assignments of $7a + 6a + 5a/6a' + 1a'' + 5a'$. A good agreement between XMP and TMPs shown in Figure 3c clearly reveals that these two bands should be assigned to the ionizations from orbitals of $7a + 6a + 5a/6a' + 1a'' + 5a$, as theoretical calculations predicted. Unfortunately, because of the low-energy resolution, it is not possible for us to assign p4 and p5 bands separately.

The XMP and TMPs for p6 are shown in Figure 3d. The He I UPS work of White et al.[56] assigned p6 to $1a''$ for the syn conformer. But the SRPES work of Bawagan et al.[57] give a different assignment of $4a'$. All the present theoretical calculations including the OVGF, P3, B3LYP methods assign p6 to the ionizations from $4a'/4a$, supporting the SRPES's result. As can be seen in BES, p6 is well resolved and thus the momentum profile of this band is much reliable. It is easy to make the clear assignment by simply comparing the XMP with TMPs for the two different assignments.[61] As shown in Figure 3d, the TMPs for $4a'/4a$ are in better agreement with XMP than that for $1a''/6a$, which largely underestimates the experiment. Hence, the present EMS work assigns p6 to the ionization of $4a'/4a$, which is consistent with the results of SRPES experiment and theoretical calculations. The orbital plots indicate that both $4a$ orbital of the skew conformer and $4a'$ of the syn conformer have electron densities predominantly distributed on the ethenyl group. Therefore, similar to HOMO, the rotation of methyl group also has small influence on the electron momentum distributions. Both of the individual TMPs for the two conformers are "p-type" with different maximum positions at $p \sim 0.5$ au for $4a$ and $p \sim 0.7$ au for $4a'$.

The XMP and TMPs for band p7 ($3a/3a'$) are shown in Figure 3e. All the TMPs are in good agreement with XMP and exhibit "sp-type" character with a secondary maximum at $p \sim 0.6$ au. The orbital plots indicate that $3a$ orbital of skew conformer and $3a'$ of syn conformer both have electron densities mainly distributed on the methyl group and C−C single bond. Thus the torsion of methyl group can obviously influence the individual momentum profiles for the two conformers of 1-butene. The TMP for $3a$ is "sp-type" in nature with a secondary maximum at $p \sim 0.65$ au, while the TMP for $3a'$ exhibits "p-type" character with a maximum at $p \sim 0.5$ au.

Bands p8 and p9 correspond to the ionizations of the two innermost valence orbitals ($2a/2a'$ and $1a/1a'$). The XMPs and TMPs for these two bands are shown in Figure 3f,g, and it can be seen that all the TMPs calculated by B3LYP method with different sized basis sets consist with each other for these inner valence orbitals. The ionizations of these two inner valence orbitals exhibit pole strengths that are significantly less than unity due to the importance of final state electron correlation effects in these ionizations. As can be seen in Figure 3f, the electron densities in position space for the $2a$ orbital of the skew conformer and the $2a'$ orbital of the syn conformer basically distribute on the C═C double bond and ethyl group. A node plane perpendicular to the middle C−C bond is obvious, and therefore both of the individual TMPs for the two conformers are of "p-type" in nature. The XMP for band p8 corresponding to $2a/2a'$ orbital exhibits an expectant "p-type" character. All the TMPs overestimate the relative intensities for this orbital, while reproducing the shape well except in the low momentum where XMP shows an obvious turn up. This turn up may also be due to the distorted wave effect for the pseudo-π orbitals. The good agreement between the XMP and TMP by B3LYP/aug-cc-pVTZ can be achieved if the TMP is scaled by a factor

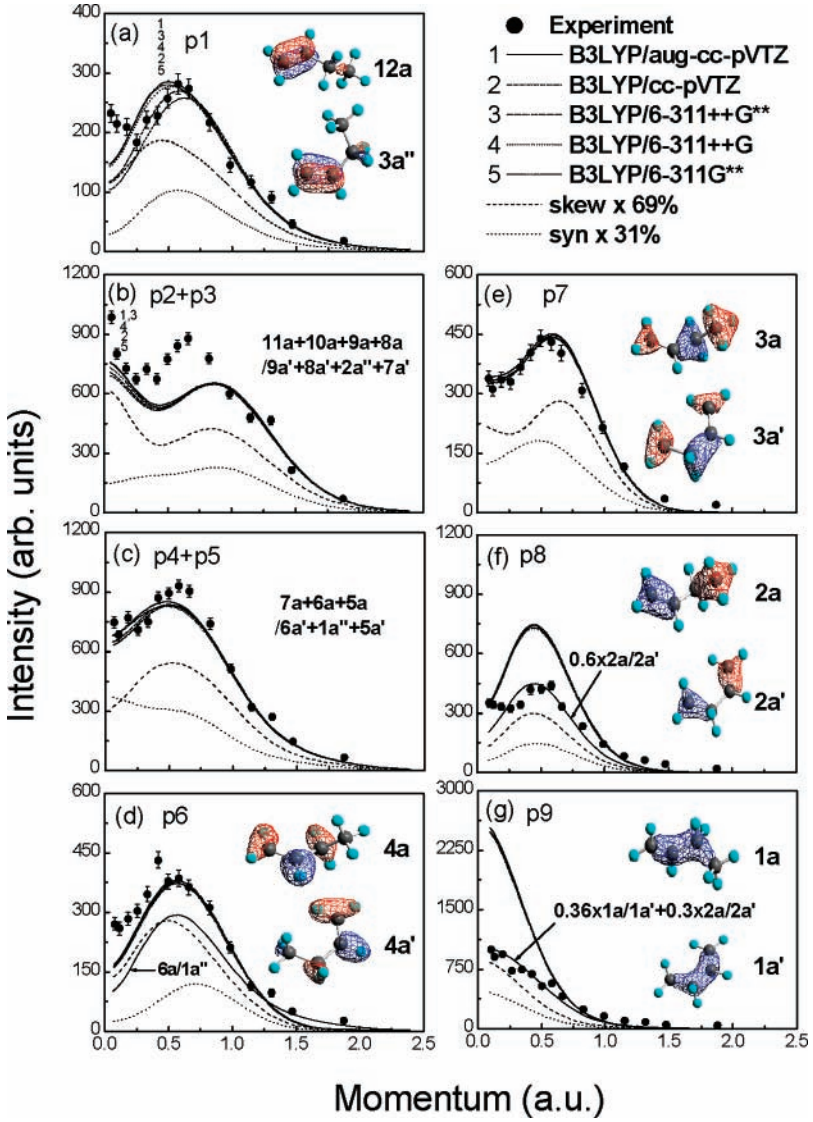

Figure 3. The experimental and theoretical momentum profiles calculated by B3LYP method with 6-311++G**, 6-311++G, 6-311G**, cc-pVTZ, and aug-cc-pVTZ basis sets for the valence orbitals of 1-butene. The total TMP is the Boltzmann-weighted summation of the individual TMPs for the skew (69%) and syn (31%) conformers.

TABLE 3: syn−skew Energy Difference (kcal/mol) for 1-Butene at Room Temperature (298 K)

	theoretical			experimental				
	CBS-Q[16]	G2[16]	MP2[a]	MW[33]	Raman[32]	NMR[35−37]	IR[31]	EMS[a]
ΔG	0.47	0.40	0.45/0.43					0.47 ± 0.20
ΔH	0.37	0.30	0.14/0.10	0.15 ± 0.15	−0.220	-0.10 ± 0.05	-0.209 ± 0.017	

[a] This work. The basis sets used in MP2 calculations are cc-pVTZ/aug-ccpVTZ.

of 0.6, which represents the pole strength for the main transition of $2a^{-1}/2a'^{-1}$.

The XMP for band p9 displayed in Figure 3g exhibits an "s-type" profile. The orbital plots in Figure 3g show that both of 1*a* orbital for the skew conformer and 1*a*′ orbital for the syn conformer mainly comprise carbon 2s components and the TMPs for 1*a*/1*a*′ are rationally of "s-type". However, even if the TMPs for 1*a*/1*a*′ are scaled by a proper factor, they still cannot well describe the XMP for this band. It is reasonable to take into account the contribution from satellite states of the $2a^{-1}/2a'^{-1}$ transition. An admixture of $0.36 \times (1a/1a') + 0.30 \times (2a/2a')$ TMP reproduces the XMP well as shown in Figure 3g, where 0.36 represents the pole strength for the main transition of $1a^{-1}/1a'^{-1}$ and 0.30 is the pole strength contributed by the $2a^{-1}/2a'^{-1}$ satellites in the energy region of band p9. The missing intensity of 2*a*/2*a*′ and 1*a*/1*a*′ is most likely distributed in the energy region beyond about 26 eV as shown in Figure 2.

C. Conformational Stability of 1-Butene. As mentioned in the Introduction, the relative stability of the conformers of 1-butene is still a controversial issue. The syn−skew relative enthalpies ΔH obtained by the previous experiments are listed in Table 3, together with the theoretically calculated syn−skew relative Gibbs free energies ΔG and enthalpies ΔH by CBS-Q and G2 methods,[16] as well as the present MP2 method with cc-pVTZ and aug-cc-pVTZ basis sets. In general, all the previous experiments[31−37] predicated that the syn conformer is more stable than the skew except the MW work,[33] while various levels of theoretical calculations predict an inverse order.

As shown in Section III. B, the rotation of methyl group in

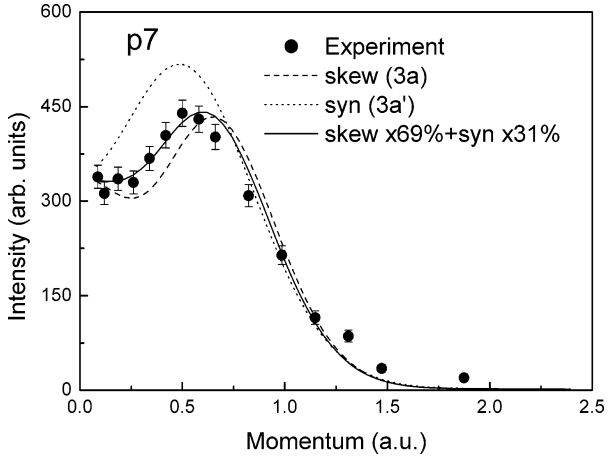

Figure 4. The experimental and theoretical momentum profiles for the ionization band of p7 for 1-butene.

1-butene that leads to the two conformers can have an obvious effect on the electron momentum profiles for some of the valence orbitals. By comparing the XMP with the weighted summation of TMPs for the skew and syn conformers, the Boltzmann-weighted abundances and thus the relative stability for conformers can be determined. It is important to select an appropriate ionization band in determining the relative abundances by EMS. As can be seen in Figure 3, among all the ionization bands, band p7 of $3a/3a'$ ionization is the best candidate that is well resolved in the BES and the individual TMPs for $3a$ and $3a'$ orbitals largely influenced by the conformational effect.

The XMP for band p7 is shown again as solid circles in Figure 4. Because 1-butene coexists in two conformers, band p7 actually contains ionizations of $3a$ (skew) and $3a'$ (syn) orbitals. The individual TMPs for $3a$ (skew) and $3a'$ (syn) orbitals calculated by B3LYP/cc-pVTZ are also plotted in Figure 4. As can be seen in the figure, neither of the individual TMP can reproduce the XMP, especially in the low momentum region below 0.6 au with TMP for $3a$ (skew) underestimating and TMP for $3a'$ (syn) overestimating the XMP. By taking relative conformational abundances of (69 ± 6)% for the skew and (31 ± 6)% for the syn, the summed TMP (solid curve in Figure 4) best reproduces the XMP. The 6% accuracy only includes the standard deviations in the least-square fitting procedure determining the abundances. In this way, the Boltzmann-weighted abundances for the two conformers of 1-butene at room temperature (298 K) are then determined indicating that the skew conformer is the preferential one, which is in consistence with the predications of the previous MW[33] work and theoretical calculations. The deduced relative conformational abundances were employed throughout Section III. B and well describe the XMPs for the complete valence orbitals of 1-butene, indicating the rationality of the results of the relative abundances.

The equilibrium conformational abundances depend on the Gibbs free energy difference ΔG of the two conformers. The conformational equilibrium constant (K_T) can be simply estimated by the following equation

$$\ln K_T = -\Delta G/RT \qquad (3)$$

where $RT = 0.592$ kcal/mol at room temperature and the Gibbs free energy has a relationship with enthalpy and entropy as $\Delta G = \Delta H - T\Delta S$. By substituting the above-gained relative conformational abundances in eq 3, a syn−skew relative Gibbs energy of 0.47 ± 0.20 kcal/mol can be obtained, which is in a good agreement with the previous CBS-Q calculations[16] (0.47 kcal/mol) and the present MP2 results (0.45 and 0.43 kcal/mol).

IV. Summary

In summary, the first EMS studies on the valence orbitals of 1-butene are reported. The XMPs are compared with the TMPs calculated by using B3LYP method with 6-311++G, 6-311G**, 6-311++G**, cc-pVTZ, and aug-cc-pVTZ basis sets. The calculated momentum profiles are generally in good agreement with the experimental ones. The strong proofs provided by the present EMS experiments and IP calculations support the assignments of the bands at 14.8 and 15.9 eV to the ionizations of $7a + 6a + 5a/6a' + 1a'' + 5a'$ and band at 18.3 eV to the ionization of $4a'/4a$ in BES. The pole strengths for the two innermost valence orbitals have also been determined.

The conformational stability of 1-butene has been investigated in the present work by EMS. The well-resolved ionization band p7 at 20.7 eV was selected to determine the relative abundances of the two conformers of 1-butene by comparison the XMP with the Boltzmann-weighted summation of the individual TMPs for the two conformers. The relative conformational abundances of (69 ± 6)% for skew conformer and (31 ± 6)% for syn conformer at room temperature were obtained and syn-skew relative Gibbs free energy of 0.47 ±0.20 kcal/mol was deduced, indicating that the skew conformer is the preferential one. The results demonstrate latent potential of EMS as an effective tool to study the relative conformational stability.

Acknowledgment. This work was supported by National Natural Science Foundation of China (Grants 10474090 and 10734040). The authors also gratefully acknowledge Professor C. E. Brion from University of British Columbia (UBC) in Canada for giving us the HEMS and RESFOLD programs.

References and Notes

(1) Zhang, M.; Huang, Z. J.; Lin, Z. J. *J. Chem. Phys.* **2005**, *123*, 134313.
(2) Ha, T. K.; Gunthard, H. H. *J. Am. Chem. Soc.* **1993**, *115*, 11939.
(3) Akasaka, T.; Wakahara, T.; Nagase, S.; Kobayashi, K.; Waelchli, M.; Yamamoto, K.; Kondo, M.; Shirakura, S.; Maeda, Y.; Kato, T.; Kako, M.; Nakadaira, Y.; Gao, X.; Caemelbecke, E. V.; Kadish, K. M. *J. Phys. Chem. B* **2001**, *105*, 2971.
(4) Shivanyuk, A.; Rebek, J., Jr. *J. Am. Chem. Soc*. **2002**, *124*, 12074.
(5) Satink, R. G.; Meijer, G.; Helden, G. von. *J. Am. Chem. Soc*. **2003**, *125*, 15714.
(6) Kenny, J. P.; Krueger, K. M.; Rienstra-Kiracofe, J. C.; Schaefer, H. F. *J. Phys. Chem. A* **2001**, *105*, 7745.
(7) Kurihara, M.; Matsuda, T.; Hirooka, A.; Yutaka, T. *J. Am. Chem. Soc*. **2000**, *122*, 12373.
(8) Dugourd, Ph.; Hudgins, R. R.; Tenenbaum, J. M.; Jarrold, M. F. *Phys. Rev. Lett.* **1998**, *80*, 4197.
(9) Anderson, K. B.; Tranter, R. S.; Tang, W.; Brezinsky, K.; Harding, L. B. *J. Phys. Chem. A* **2004**, *108*, 3403.
(10) Civcir, P. Ü.; *J. Mol. Struct. (THEOCHEM)*. **2000**, *532*, 157.
(11) Naumkin, F. Y.; McCourt, F. R. W. *J. Chem. Phys.* **1998**, *108*, 9301.
(12) Tian, S. X.; Xu, K. Z. *Chem. Phys*. **2001**, *264*, 187.
(13) Piuzzi, F.; Mons, M.; Dimicoli, I.; Tardivel, B.; Zhao Q. *Chem. Phys*. **2001**, *270*, 205.
(14) Chen, Y. Z.; Mohan, V.; Griffey, R. H. *Phys. Rev. E* **2000**, *61*, 5640.
(15) Gould, I. R.; Burton, N. A.; Hall, R. J.; Hillier, I. H. *J. Mol. Struct. (THEOCHEM)* **1995**, *331*, 147.
(16) Murcko, M. A.; Castejon, H.; Wiberg, K. B. *J. Phys. Chem.* **1996**, *100*, 16162.
(17) Abu-samha, M.; B¢rve, K. J.; Sæthre, L. J.; Thomas, T. D. *Phys. Rev. Lett.* **2005**, *95*, 103002.
(18) Saha, S.; Wang, F.; Falzon, C. T.; Brunger, M. J. *J. Chem. Phys*. **2005**, *123*, 124315.
(19) Kodama, T.; Ozawa, N.; Miyake, Y.; Sakaguchi, K.; Nishikawa, H.; Ikemoto, I.; Kikuchi, K.; Achiba, Y. *J. Am. Chem. Soc*. **2002**, *124*, 1452.

(20) Nagashima, N.; Kudoh, S.; Takayanagi, M.; Nakata, M. *J. Phys. Chem. A* **2001**, *105*, 10832.
(21) Minoura, Y.; Nagashima, N.; Kudoh, S. Nakata, M. *J. Phys. Chem. A* **2004**, *108*, 2353.
(22) Falzon, C. T.; Wang, F. *J. Chem. Phys*. **2005**, *123*, 214307.
(23) Galasso, V. *J. Chem. Phys.* **1995**, *102*, 7158.
(24) Woo, H. K.; Zhan, J. P.; Lau, K. C.; Ng, C. Y.; Cheung, Y. S. *J. Chem. Phys.* **2002**, *116*, 8803.
(25) Woo, H. K.; Lau, K. C.; Zhan, J. P.; Ng, C. Y.; Li, C. L.; Li, W. K.; Johnson, P. M. *J. Chem. Phys.* **2003**, *119*, 7789.
(26) Wiberg, K. B.; Ellison, G. B.; Wendoloski, J. J.; Brundle, C. R.; Kuebler, N. A. *J. Am. Chem. Soc.* **1976**, *98*, 7179.
(27) Mannfors, B.; Sundius, T.; Palmo, K.; Pietila, L. O.; Krimm, S. *J. Mol. Struct*. **2000**, *521*, 49.
(28) Bauschlicher, C. W., Jr. *Chem. Phys. Lett*. **1995**, *239*, 252.
(29) Jungwirth, P.; Bally, T. *J. Am. Chem. Soc*. **1993**, *115*, 5783.
(30) Fronzoni, G.; Lisini, A. *Chem. Phys*. **1996**, *207*, 1.
(31) Bell, S.; Drew, B. R.; Guirgis, G. A.; Durig, J. R. *J. Mol. Struct.* **2000**, *553*, 199.
(32) Durig, J. R.; Compton, D. A. C. *J. Phys. Chem*. **1980**, *84*, 773.
(33) Kondo, S.; Hirota, E, Morino, Y. *J. Mol. Spectrosc.* **1968**, *28*, 471.
(34) Gallinella, E.; Cadioli, B. *Vib. Spectrosc.* **1997**, *13*, 163.
(35) Bothner-By, A. A.; Naar-Colin, C. *J. Am. Chem. Soc.* **1961**, *83*, 231.
(36) Bothner-By, A. A.; Narr-Colin, C.; Günther H. *J. Am. Chem. Soc*. **1962**, *84*, 2748.
(37) Karabatsos, G. J.; Taller, R. A. *Tetrahedron*. **1968**, *24*, 3923.
(38) McCarthy, I. E. Weigold, E. *Rep. Prog. Phys.* **1991**, *54*, 789.
(39) Mathers, C. P.; Gover, B. N.; Ying, J. F.; Zhu, H.; Leung, K. T. *J. Am. Chem. Soc*. **1994**, *116*, 7250.
(40) Ying, J. F.; Zhu, H.; Mathers, C. P.; Gover, B. N., Banjavčić M. P.; Zheng, Y.; Brion, C. E.; Leung, K. T. *J. Chem. Phys*. **1993**, *98*, 4512.
(41) Mathers, C. P.; Ying, J. F.; Gover, B. N.; Leung, K. T. *Chem. Phys*. **1994**, *184*, 295.
(42) Chuaqui, M. H.; Mei, L.; Mathers, C. P.; Allison, M. L.; Ying, J. F.; Leung, K. T. *J. Chem. Phys*. **1995**, *102*, 90.
(43) Neville, J. J.; Zheng, Y.; Brion, C. E. *J. Am. Chem. Soc*. **1996**, *118*, 10533.
(44) Zheng, Y.; Neville, J. J.; Brion, C. E. *Science* **1995**, *270*, 786.
(45) Deleuze, M. S.; Pang, W. N.; Salam, A, Shang, R. C. *J. Am. Chem. Soc*. **2001**, *123*, 4049.
(46) Wang, F.; Downton, M. *J. Phys. B: At. Mol. Opt. Phys.* **2004**, *37*, 557.
(47) Yang, T. C.; Su, G. L.; Ning, C. G.; Deng, J. K.; Wang, F.; Zhang, S. F.; Ren, X. G.; Huang, Y. R. *J. Phys. Chem. A* **2007**, *111*, 4927.
(48) Yang, B. X.; Chen, X. J.; Pang, W. N.; Chen, M. H.; Zhang, F.; Tian, B. L.; Xu, K. Z. *Acta. Phys. Sin.* **1997**, *5*, 862.
(49) Duffy, P.; Chong, D. P.; Casida, M. E.; Salahub, D. R. *Phys. Rev. A* **1994**, *50*, 4707.
(50) Frisch, M. J.; Trucks, G. W.; Schlegel, H. B.; Scuseria, G. E.; Robb, M. A.; Cheeseman, J. R.; Montgomery, J. A., Jr.; Vreven, T.; Kudin, K. N.; Burant, J. C.; Millam, J. M.; Iyengar, S. S.; Tomasi, J.; Barone, V.; Mennucci, B.; Cossi, M.; Scalmani, G.; Rega, N.; Petersson, G. A.; Nakatsuji, H.; Hada, M.; Ehara, M.; Toyota, K.; Fukuda, R.; Hasegawa, J.; Ishida, M.; Nakajima, T.; Honda, Y.; Kitao, O.; Nakai, H.; Klene, M.; Li, X.; Knox, J. E.; Hratchian, H. P.; Cross, J. B.; Bakken, V.; Adamo, C.; Jaramillo, J.; Gomperts, R.; Stratmann, R. E.; Yazyev, O.; Austin, A. J.; Cammi, R.; Pomelli, C.; Ochterski, J. W.; Ayala, P. Y.; Morokuma, K.; Voth, G. A.; Salvador, P.; Dannenberg, J. J.; Zakrzewski, V. G.; Dapprich, S.; Daniels, A. D.; Strain, M. C.; Farkas, O.; Malick, D. K.; Rabuck, A. D.; Raghavachari, K.; Foresman, J. B.; Ortiz, J. V.; Cui, Q.; Baboul, A. G.; Clifford, S.; Cioslowski, J.; Stefanov, B. B.; Liu, G.; Liashenko, A.; Piskorz, P.; Komaromi, I.; Martin, R. L.; Fox, D. J.; Keith, T.; Al-Laham, M. A.; Peng, C. Y.; Nanayakkara, A.; Challacombe, M.; Gill, P. M. W.; Johnson, B.; Chen, W.; Wong, M. W.; Gonzalez, C.; Pople, J. A. *Gaussian 03*, revision B.04; Pittsburgh, PA, 2003.
(51) Becke, A. D. *J. Chem. Phys.* **1993**, *98*, 5648.
(52) Duffy, P.; Casida, M. E.; Brion, C. E.; Chong, D. P. *Chem. Phys*. **1992**, *159*, 347.
(53) Niessen, W.; von, Schirmer, J.; Cederbaum, L. S. *Comput. Phys. Rep.* **1984**, *1*, 57.
(54) Ortiz, J. V. *J. Chem. Phys.* **1996**, *104*, 7599.
(55) Wang, F.; Pang, W. N.; Huang, M. *J. Electron. Spectrosc. Relat. Phenom.* **2006**, *151*, 215.
(56) White, R. M.; Carlson, T. A.; Spears, D. P. *J. Electron. Spectrosc. Relat. Phenom.* **1974**, *3*, 59**.**
(57) Bawagan, A. D. O.; Desjardins, S. J.; Dailey, R.; Davidson, E. R. *J. Chem. Phys*. **1997**, *107*, 4295.
(58) Brion, C. E.; Zheng, Y.; Rolke, J.; Neville, J. J.; McCarthy, I. E.; Wang, J. *J. Phys. B: At. Mol. Opt. Phys.* **1998**, *31*, L223.
(59) Rolke, J.; Zheng, Y.; Brion, C. E.; Chakravorty, S. J.; Davidson, E. R.; McCarthy, I. E. *Chem. Phys*. **1997**, *215*, 191.
(60) Ren, X. G.; Ning, C. G.; Deng, J. K.; Zhang, S. F.; Su, G. L.; Huang, F.; Li G. Q. *Phys. Rev. Lett.* **2005**, *94*, 163201.
(61) Shan, X.; Chen, X. J.; Zhou, L. X.; Li, Z. J.; Liu, T.; Xue, X. X.; Xu, K. Z. *J. Chem. Phys.* **2006**, *125*, 154307.